

UDC 621

ALGORITHM OF CLASSIFICATION OF SHAFT ORBITS

D. KECHIK, PhD I. DAVYDOV, I. LOSHCININ, K. ZHUKOVSKIY
(Belarusian State University of Informatics and Radioelectronics, Minsk)

Classification of spatial patterns of shaft orbits is studied in this paper. Recent methods of signal processing, such as spectral interference frequency refinement method, Mallat scattering transform were tested for task of obtaining patterns, informative features extraction and classification. Strong dependence on fluctuations of signal parameters and significant variability of spatial patterns has been discussed. Effectiveness of ranking of patterns using different approaches has been estimated using computational modelling and natural experiments. Preprocessing of signal and informative features has been considered. Approach of discrimination of different misalignment types and severities, based on rate of occurrence of classes of spatial patterns, has been proposed, its effectiveness has been demonstrated.

Keywords: *pattern recognition, frequency domain, spatial domain, time synchronous averaging, phase processing, vibrational diagnosing, scattering transform, wavelet transform, convolutional network, support vector machine.*

Introduction. In normal and various defect states displacement of shaft is periodical process. Measurement of trajectory of center of shaft at its end, or shaft orbit, has been used for diagnosing of rotary equipment for a long time. Shaft displacement in orthogonal directions carry full information about dynamical forces occurred in rotary system [1; 2]: shaft and related plain bearings [3–6], rolling bearings [1], couplings [3–6]. Thus, shaft orbit related with machine state unambiguously [2]. It shows processes in system pictorially [2] and is convenient for experienced expert. Idea of spatial averaged shaft orbits is close to time synchronous averaging (TSA) [7–9] of signal of vibration for extraction of patterns of signal that are informative features of equipment state. Both methods require synchronization with shaft rotation frequency. It can be usually achieved by tachometer. Another approach is to estimate instantaneous shaft rotation frequency using vibration signal [10; 11]. Vibration is assumed to be stationary, and temporal or spatial patterns can be obtained by averaging of signal frames of length of shaft revolution period. Signals of vibration observed under condition of varying speed can be resampled with equiangular step [10; 11] to obtain stationary signals and recover spectral, temporal and spatial informative features could be selected by conventional methods.

To display shaft orbit, let averaged vertical radial displacement be on Y axis and averaged horizontal radial displacement be on X axis. This idea is close to idea of Lissajous figures that are images of orthogonal oscillations [12; 13]. Unambiguous dependence of figure form on their phase and frequency relations has been shown [13]. Under frequency relations ratios of frequencies of present components of signals in the both channels to the frequency of fundamental frequency is understood. Phase relations term means relative values of initial phases of the components of signals in both channels as well as phase shift between channels. Fundamental frequency (FF) is the first harmonic of the signal, shaft rotation frequency.

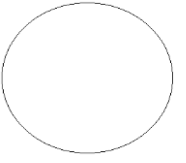
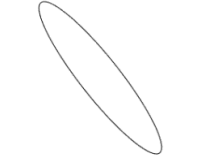


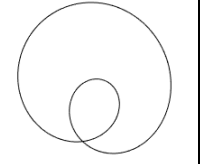
The commonly used method of vibrational diagnosing is analysis of amplitude spectrum of vibrational signal and its envelope. Fourier transform (FT), of fast FT (FFT) is the most appropriate method: its implementation using modern computational technique is simple, basis functions (sinus and cosine) are correspond to oscillations of real mechanical system [14] and impulse response of linear system, it has high frequency resolution and noise immunity: even a component of low power is discriminable at wideband noise or/and harmonic of higher power and close frequency. Amplitudes of harmonics whose frequencies are multiple to FF are selected as informative features. Relations of the amplitudes and their growth is related with defect kind and its severity (class of equipment state) [15].

Shaft orbit can consider also phase relations (not values of initial phases that are random, but their relations [13]), non-synchronous vibration (usually at 0.4...0.5 FF), wideband vibration. Variability, sensitivity to small variation of parameters, relations of orbit classes and equipment state classes are studied in this paper. Recognition of spatial patterns of shaft orbit of equipment having misalignment has been studied in this paper. The main purpose of the paper is to investigate relations of defect kind as well as its severity with class of pattern, appropriate selection of spatial patterns among highly varied and distorted orbits and application of recent methods of signal processing for analysis of vibration and images. Classes of patterns described in literature and observed at testbed are considered. The rest of paper is organized as the following: in the Section 2 learning dataset (patterns obtaining) is discussed, the Section 3 describes pattern extraction. Pattern recognition and classification of shaft trajectories is discussed in the Section 4. The last section concludes the paper.

Dataset. Review of literature sources has showed that relations of shape of orbit and defect is different in different sources. Circle (C) [16] or Ellipse (E) [17, 18] orbits may indicate normal state of equipment. Elliptical [16–18] or close to circle [2] orbits may appear if shaft imbalance is present. Trajectory of misaligned

shaft may be elliptical [2] or have more complex form, named “Eight” (8), “Heart” (H) or “Tornado” (T) [16], the similar shapes are reported in [4] for various faults. Classes of pattern are often described as what they look like (e.g., Tornado, Heart) and what elements they are consist of (e.g., number of loops that may be important to explain physical processes, see [3]). We will keep this tradition next. Examples of classes adduced in literature are presented in table 1.

Table 1. – Examples of shaft orbits described in different sources

Class	Circle	Ellipse	Eight	Heart	Tornado
Image					

Misalignment can be described in two partial cases:

- angular misalignment (figure 1, *a*) is a state when axes of joined shafts are not parallel;
- parallel misalignment (figure 1, *b*) is a state when axes of joined shafts are parallel and do not lie on the same straight line.

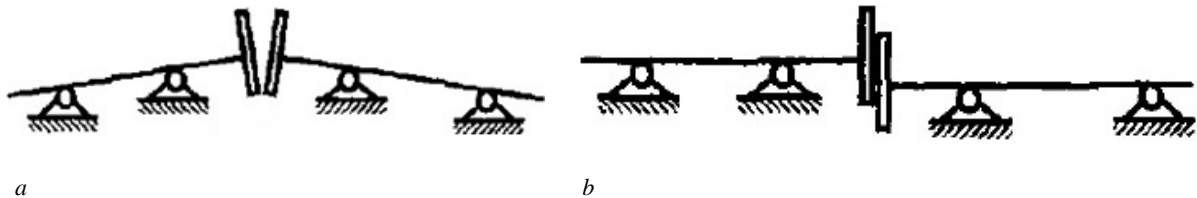


Figure 1. – Types of misalignment [19]

More generally, both types of misalignment can appear simultaneously, but we don't discuss this complex case. Lack of attention is paid to difference between kinds of misalignment in the papers devoted to studying of shaft orbits, despite even amplitude spectrum significantly differs that affects on orbit shape: the second (more rarely the third) harmonic grows faster at parallel misalignment rather than at angular misalignment [3; 5]. Sources that describe features in amplitude spectrum in detail usually do not pay attention to phase relations, and shaft orbits is only feature that experienced expert can analyze to obtain full information. Make unambiguous decision relying just on amplitude spectrum is not possible [3; 5]. Axial vibration may be additional source of information [5; 6; 20], but it is usually ignored. Growth of axial vibration may indicate misalignment [6; 20], but it is not ambiguous.

It is important to detect incipient defect and predict remaining resource of equipment. Tracking of amplitude values and their relations [15], statistical characteristics of signal [21] is used to estimate equipment state more accurate. Any changing of spatial pattern of shaft orbit may indicate its malfunction [22]. Spatial pattern is also developing when severity of the defect increases: shaft orbit is reported to be elliptical at the early stage of misalignment and become Eight further [23]. Estimation of defect severity, tracking and prediction of its evolution are needed to schedule maintenance of equipment more rationally [21; 23]. Then, we study dependence of spatial patterns of shaft orbit on defect kind and its severity using testbed vibration as an example.

Two datasets of vibration observed at bearing housing of equipment having parallel [24] and angular [25] misalignment of different severity were recorded. Each of them contains vibration signals observed under conditions of both kinds of misalignment of different severity in three orthogonal directions: radial vertical (V), radial horizontal (H), axial (A). Signals were observed at bearing housing of testbed using three orthogonal accelerometers. Bearing was separated from motor by jaw coupling. Severity and type of misalignment was regulated by special apparatus that shifted and rotated motor. It is notable that foundation of testbed was not rigid that is not typical for industrial equipment.

Pattern extraction. Traditionally, shaft orbits were obtained using laser (basics), proximity sensors [12; 18]. Accuracy of vibration sensors has been increased significantly. In this paper displacement of shaft is proposed to be obtained using accelerometers that are mounted in perpendicular directions. Acceleration signal is integrated twice to obtain displacement signal. Sensors were mounted on the bearing housing. Vibration contains a lot of components of different nature, and the components produced by shaft and its interaction with other elements should be selected. Components related with shaft and coupling defects are multiple to FF. Faulty plain bearing can produce multiples to FF and its half or 0.1FF in the case of lubrication defects such as oil whirl [26]. Frequencies of the most of components produced by rolling bearing are also multiple to FF [15; 27]. Two controversial

conditions must be met: suppression of wideband and harmonic noise and passing all informative wideband and narrowband components. For analysis of spatial patterns low frequencies band (0...200 Hz) as well as notch filtrated narrow bands may be selected [22]. Harmonic components of vibrational signal at low frequencies are coherent with FF [14; 28]. If FF does not variate significantly, energy of components related to shaft is concentrated in narrow band. Selection of the components using FT is appropriate [11; 21; 29]. Fourier filtration is a procedure of consequent FT of signal, windowing of complex spectrum, applying of inverse FT [29] and can be realized as [11]:

$$s_{out}(t) = \Re\{F^{-1}(Y(f) \cdot W(f_1, f_2)), W(f_1, f_2) = \begin{cases} 1, & \text{if } f_1 \leq f \leq f_2, \\ 0, & \text{otherwise,} \end{cases} \quad (1)$$

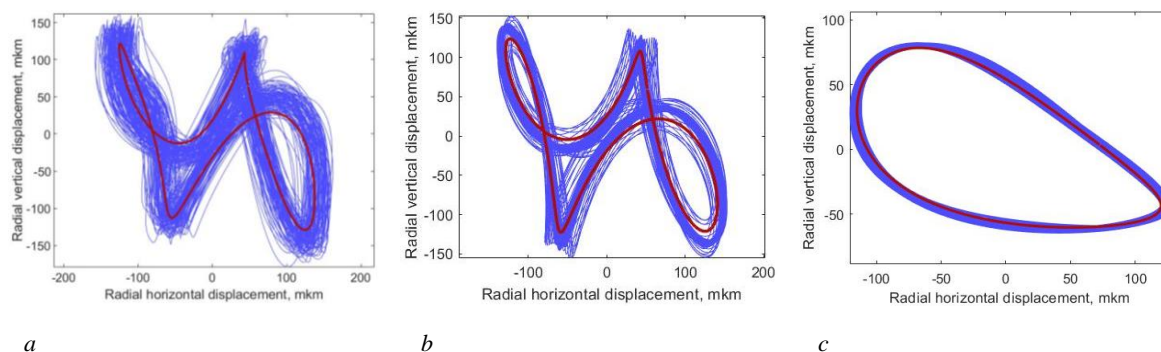
where $F^{-1}(x)$ is inverse FT;

$Y(f)$ is one sided spectrum of input signal;

$W(f_1, f_2)$ is rectangular window.

The first three harmonics of shaft rotation frequency carry information about presence and severity of both kinds of misalignment [3; 5] and should be selected. Shaft rotation frequency was refined for each signal of dataset using spectral interference method. The method is used to detect multiple frequencies at mixture of polyharmonic signal and wideband and harmonic noise. Shaft speed is estimated with high accuracy (less than 1%), then we can select narrow frequency bands of harmonics of FF. The method is used to detect automatically harmonics of FF that are prominent enough, are not splitted or leaked and are multiple to FF with high accuracy [11]. Then, we select the narrow bands in the vicinity of detected harmonics using Fourier filtration. Hereinafter, we denote multiple to FF components of vibration as nX (1X, 2X, ...), where $n = 1, 2, \dots$ is number of harmonic.

Shaft orbit is generated as Lissajous figure. We can plot filtrated signal of horizontal direction sensor along X axis and filtrated signal of vertical direction sensor along Y axis. Obtained figure is smeared and open-ended due to residual noise and deviations of frequency, as it has been shown at figure 2 on example of vibration of parallel misaligned testbed and in [12]. Signals should be averaged to obtain spatial pattern. Filtrated signals, consisting of selected harmonics and negligible residual noise, were averaged in the same manner as it is assumed using TSA method [7; 8]. Each of the signals was divided at temporal windows of length of the FF period. Tachometer signal, or keyphasor, is usually used to determine moments of full shaft revolution. Here in this paper, we divide the signal on equal windows of length of average period of filtrated 1X. It is based on assumptions of high stationarity of the signal and high SNR of selected 1X signal. Additionally, orbit images were obtained applying technique to vibration filtrated in range of 0...200 Hz. The patterns were sustainable in both cases. Trajectories obtained by limitation of harmonics number (1X and 2X) were not variated strong in case of angular misalignment depending on its severity, but orbits observed under parallel misalignment variated under different defect severity and were not similar to angular misalignment results.







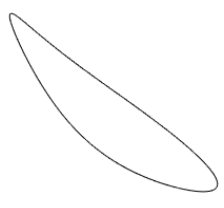
a – using low-pass Fourier filtration; b – using selection of 3 narrow band components; c – using selection of 2 components

Figure 2. – Shaft orbit and its average pattern (thick line) obtained in different way

Pattern recognition. Monitoring of evolution of informative features of defects is highly recommended [3; 15; 21; 23] to detect incipient defects, evaluate equipment state more accurate and then minimize maintenance costs. Evolution of informative features in frequency domain is well described [3]. Shaft orbits are also depending on severity of defect. For example, spatial pattern of misalignment evolves from Ellipse to Eight [23]. Shaft orbit may be distorted under various conditions [3]. Variation of shape of shaft trajectory is recommended to be monitored depending on variation of speed, load or machine process parameters [22]. Thus, dependence of shaft orbit on severity of defect should be considered when classes of shaft orbit are selected.

On the basis of literature sources (e.g. [3]) and results of numerical and natural (observed at testbed orbits are available [30]) modelling one can reveal, that select classes of patterns relying on similarity of their form unambiguously is difficult, e.g., variability of form is discussed in [3]. Number of figures are similar to described in sources classes having distortions of different severity (quantitative difference) or another geometry (e.g., degenerated loop, qualitative difference). For example, observed at experiment on testbed transient classes of orbits are presented in table 2.

Table 2. – Examples of distorted and transient classes

Class	Transition of Ellipse to Eight	Transition of Ellipse to Eight	Degenerated Eight	Degenerated Ellipse	Distorted Ellipse
Image					

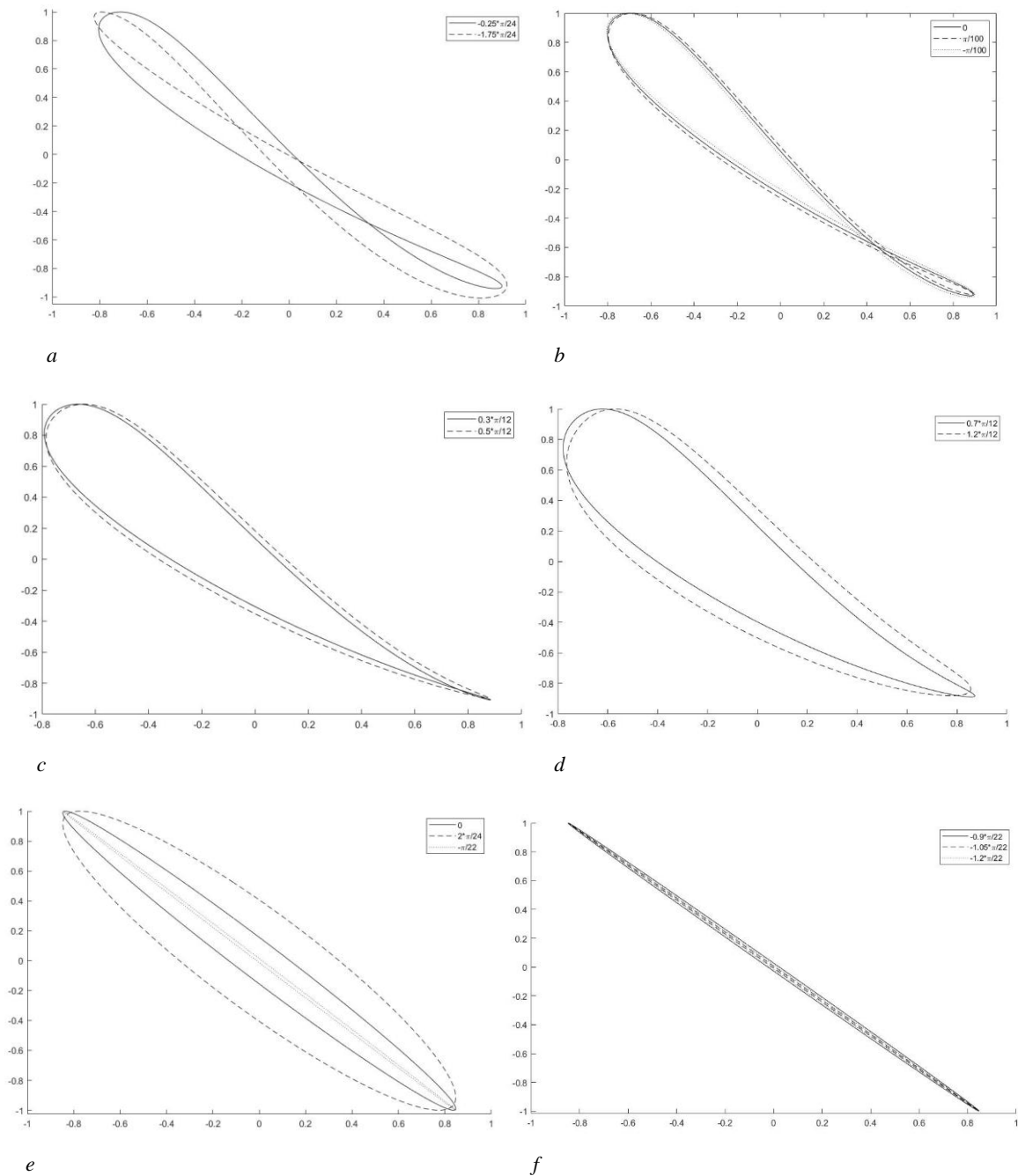
Distortions and translations between classes were reproduced numerically. Observed pattern close to translation class was selected. Three harmonics of FF were discriminated in radial horizontal and vertical channels, average amplitudes $A_{x,k} = \{105.17, 12.92, 2.59\}$, $A_{y,k} = \{124.19, 7.95, 5.53\}$ and initial phases $\varphi_{x,k} = \{3.07, -0.72, -3.23\}$, $\varphi_{y,k} = \{0.08, -0.41, 0.12\}$ were estimated as modulus and angle of analytical signals. Phase of 1X of the second channel varied to adjust shape of the pattern to obtain observed interested cases. Results are depicted at figure 3. New classes were introduced: Little_loop (figure 3, b) quantitatively differs from Eight (figure 3, a), Leaf (figure 3, c) qualitatively differs from Eight, the less loop is degenerated) Infusoria (figure 3, d) quantitatively differs from Leaf, both classes are transient to Ellipse.

It is clear that even little fluctuations of parameters of vibration caused by small fluctuations of operating mode conditions can lead to significant qualitative or quantitative changes of pattern. Significant influence of these changes on classification results has been shown by results of numerical modelling. Classes of patterns introduced before were generated. Phase of 1X component varied to produce variety of pattern shape as it has been shown at figure 3. Circle and Ellipse (figure 3, e) were generated as result of averaging harmonic signals in both channels with different shift. Ellipse_degenerated (figure 3, f) class represents the case when phase shift between channels goes to zero. Heart and Tornado classes were reproduced as Lissajous figure of two biharmonic signals.

To understand how one can rank real patterns for training of classifier, numerical experiment has been conducted. The purpose was to test three strategies of classification: ranking of quantitatively different patterns as distinct classes, ranking them as the same class, ranking qualitatively different patterns as the same class. Three datasets of images were generated. Each class of patterns contained 100 elements. Shape of patterns was varied in range has been shown at figure 2. Each of datasets was randomly divided into training (25%) and testing (75%) sets, informative features were obtained using Mallat scattering transform (see Appendix A). Classification of patterns using Support Vector Machine (see Appendix B) was tested at independent testing set. The first dataset contained patterns of different classes that are quantitatively and qualitatively different: Circle, Ellipse, Ellipse_degenerated, Eights, Little_loop, Leaf, Hearts, Tornado, Infusoria. Other datasets contained classes consists of patterns of distinct classes: elements that have only quantitative differences (Eight and Little_loop, Leaf and Infusoria, Ellipse and Ellipse_degenerated), or qualitative differences (Eight and Little_loop and Leaf). Accuracy of classification in all three cases approached 99% if training set amounted 15% or more of all dataset.

Learning on incomplete training set has been tested. Training set contained only 15 elements of a few classes (Circle, Ellipse, Eights, Hearts, Tornado). Testing set contained 100 elements of the same classes and Ellipse_degenerated, Little_loop, Leaf and Infusoria classes generated independently. Quantitatively different from Eight class Leaf and Infusoria were classified as Ellipse. As we noted above, signals with close amplitude and phase relations can produce dissimilar patterns, similar patterns can be produced by signals even with different number of components. Little_loop has been recognized as Eights. Ellipse_degenerated was mostly (77%) classified as Eights, the rest 23% were classified as Heart despite they have no visible similarity. If we add Leaf class to learning set, Infusoria classified Leaf. Little_loop was classified as Eight (78%) or Leaf (22%). Geometric similarity of patterns does not guarantee that they will be closer in space of informative features.





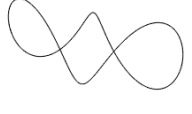
Classification of Additionally, stability of Mallat scattering transform to rotations has been tested. Testing set consisted of rotated by 90 degrees patterns of training set. Accuracy of their classification amounted 76%. Quantitatively and qualitatively different patterns can be ranked as the same class during training of classifier. Even small variation of testing pattern can lead to misclassification. Results of numerical experiments illustrated strategy of ranking real patterns for training of classifier. Classes of images should capture variation of patterns of the same equipment state and difference of patterns along defect severity increasing.





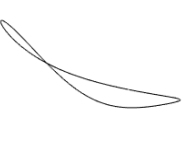


**Figure 3. – Introduced numerical modelled classes of patterns.
Each line is according to phase shift of 1X signed in legend**

Observed at testbed orbits are presented in table 3. Only regular occurred patterns were selected for each class. Classifier has been trained on images of orbits in horizontal-vertical (HV) plane. Classification of patterns in HV plane, horizontal-axial (HA) and vertical-axial (VA) planes (for vertical parallel misalignment only) has been proposed [30]. Patterns of both horizontal and vertical angular misalignment and horizontal parallel misalignment in HV plane were classified successfully. Accuracy of classification of images amounted 92% if number of elements of training set was 0.25 of number of all elements (9–15 elements). Number of patterns of angular misalignment sets were rated as introduced before classes: Leaf, Eight and Little_loop, and classifier has failed to select patterns of these classes from set of real data due to variation of form of orbits, that is consistent with numerical experiments. Classes D, H, Glasses and Rhomb contained highly varied patterns. Classes Pretzel2 and Distorted_Eight captured small distortions that improved discrimination of equipment state classes. High accuracy was achieved after training of classifier on real data. Accuracy of classification of testing set approached 95%. Patterns of vertical parallel misalignment were more stable in HA and VA planes depending on severity.

Table 3. – Examples of observed at testbed classes of patterns

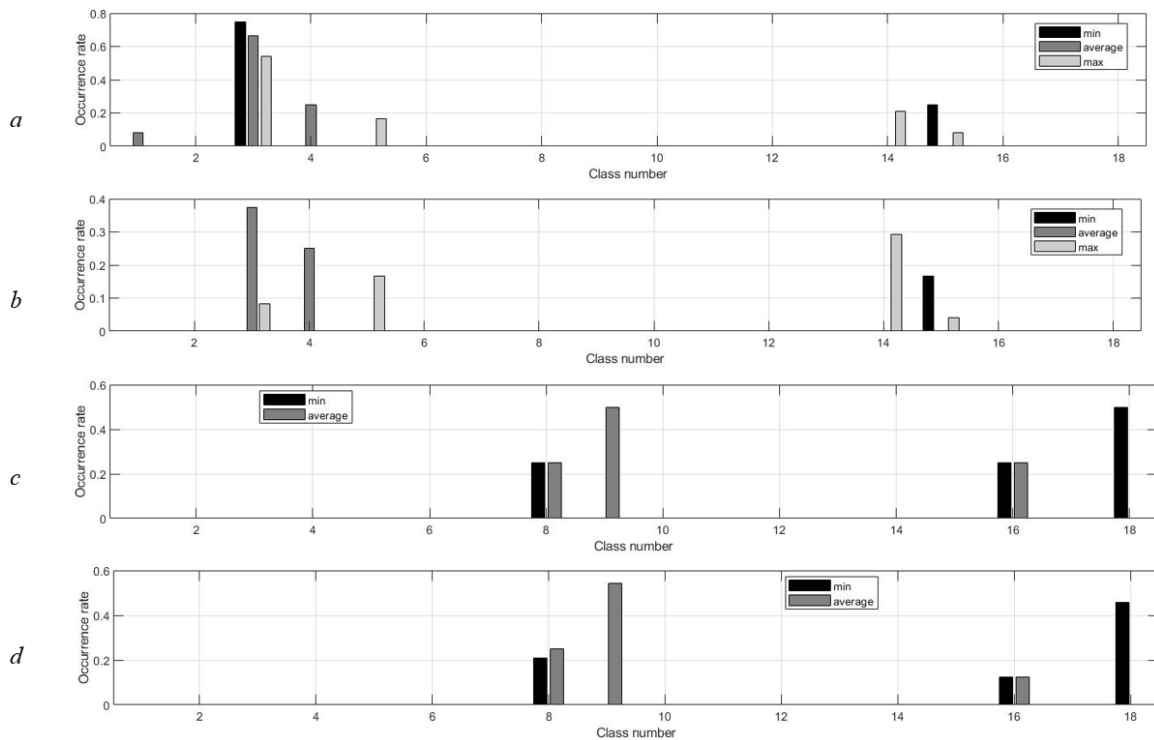
Class	Pretzel	Pretzel2	Worm	H	Glasses
Image					

End of Table 3

Class	Banano	D	Distorted_Eight	H_Vertical parallel1	Rhomb
Image					

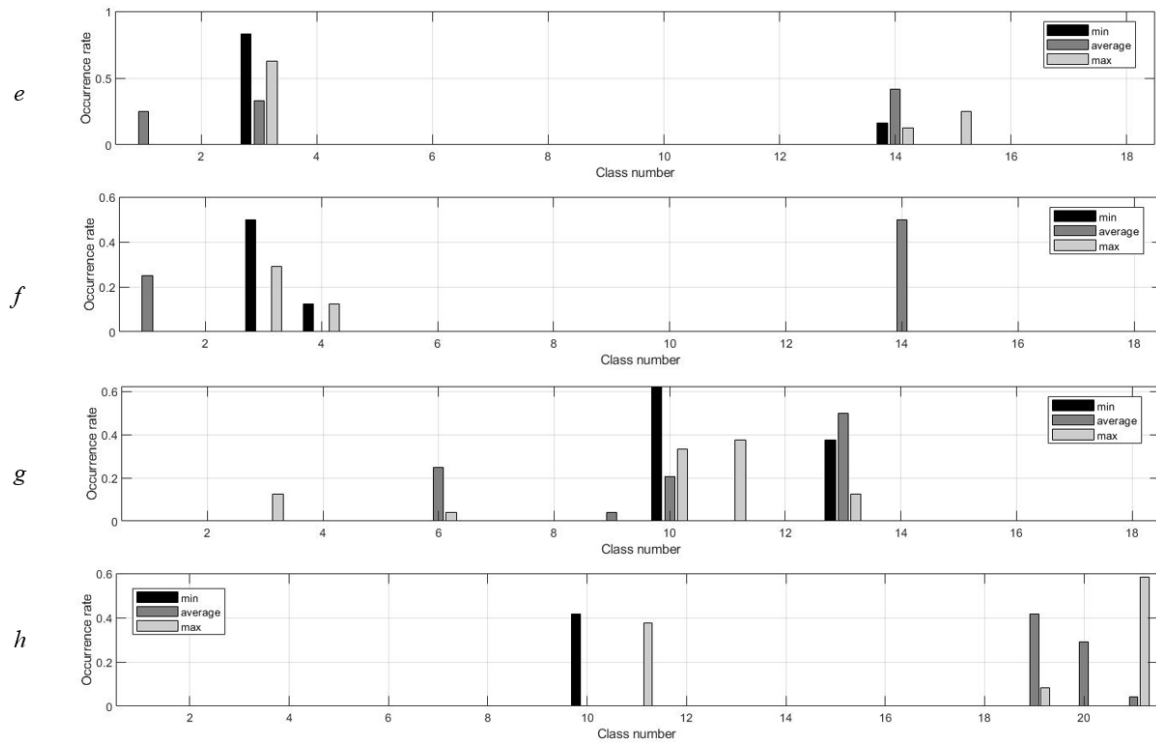
Accuracy of classification of manually ranked patterns was 89% for horizontal angular misalignment set, 98% for horizontal parallel and only 72% for vertical angular misalignment sets if training set amounted 25% of dataset. If images were ranked by classes of equipment state, accuracy significantly decreased and amounted 64%. Training set should be the half of dataset to achieve 86% accuracy. Rate of occurrence (estimated by classifier and by manual classification proposed in [30]) of each pattern of shaft orbit across each of equipment state class is presented at figure 4. Each column is a number of observations of the current defect severity that were classified as the current class of orbit divided by total number of observations of the current severity. Severities of the current defect are denoted by color of column. Classes were ordered along of X axis in the following way:

'Banano', 'CIRCLE', 'D', 'Distorted_Eight', 'Eight_angular', 'Ellipse', 'Ellipse_degenerated', 'Glasses', 'H', 'H_Vertical parallel1', 'H_Vertical parallel2', 'Hearts', 'Infusoria', 'Leaf_angular', 'Little_loop__angular', 'Pretzel', 'Tornado', 'Worm', 'Rhomb' (HA plane), 'Pretzel2' (VA plane), 'Pretzel3' (VA plane).



a, b – horizontal angular misalignment; *c, d* – horizontal parallel misalignment;
a, c, – classes detected by SVM; *b, d*, – manually classified patterns

Figure 4. – Occurrence rate of each class of pattern across equipment state classes (beginning)



e, f – vertical angular misalignment; *g, h* – vertical parallel misalignment;
e, g – classes detected by SVM; *f, h* – manually classified patterns

Figure 4. – Occurrence rate of each class of pattern across equipment state classes (end)

As we can see, classes of patterns are discriminable as well as classes of equipment state. The same classes of patterns occurred with different rates in cases of distinct severities of the same defect. It is notable that classifier ranks *each* image, i.e., patterns that were not similar to any class of image were classified too, and results automatic classification may be corrupted. Used in this paper library of SVM can be used for estimation of probabilities of each class of pattern, then probability threshold can be adjusted to trade-off between reduction of number of wrong classified images and missing of potentially right classified images.

Conclusions. Lissajous figures were used for visual observation of phase relations of modulated signals [13]. Occurrence rate of spatial patterns is related with type and severity of defect. But patterns depend strong on fluctuations of amplitudes and phases, variation of conditions of equipment operation. Defining of classes of patterns can be complicated. Learning of classifiers on synthesized patterns is not reliable. Reduction of number of informative features is appropriate for automatic signal processing, then expression of amplitude, frequency and phase relations of the components of signals of the orthogonal sensors is more preferable. Phase shifts between harmonics of the same signal as well as between signals of distinct sensors can be used. Phase invariant or phase quasi-invariant are relative phase measurements called inter-component phase relations (ICPR) that characterize phase shift between harmonics of signal caused by influence of wave propagation medium [31]. ICPR can be informative features in various fields [13; 31; 32], it was demonstrated to be effective for discrimination of severity of parallel equipment [31]. Analysis of axial vibration is not widely discussed, but amplitude and phase relations of axial and radial vibration can be useful to discriminate both types of misalignment and estimate its severity. Applied recent methods of signal processing can improve shaft orbit analysis (both automated and manual) as well as analysis of amplitude and phase relations of multichannel vibrational signal.

Appendix A

Mallat scattering transform. The transform is based on idea of Scattering Network. It consists of a few layers. Linear operator is applied at each layer to signal propagated from the previous one. Non-linear operator is applied to output data of each layer. It can be interpreted as convolutional neural network, whose filters are predefined, but not learned [33; 34]. Combination of both of operators is called propagator. Non-linear operator is modulus, wavelet transform is used as a linear operator. As a result, propagator is non-expansive to distortions, is invariant to translations and rotation. Wavelet transform at each layer is convolution of input signal with translated and rotated mother wavelet [35]:

$$\Psi_{j,\theta}(p) = 2^{-2j} \psi(2^{-j} r_{\theta} p). \tag{2}$$

The operator Φ is called nonexpansive if the following condition holds [33; 34]:

$$\forall (f, h) \in \mathbf{L}^2(\mathbb{R}^d)^2 \quad \|\Phi(f) - \Phi(h)\|_H \leq \|f - h\|, \quad (3)$$

where $\|f\|$ denotes norm of f in Hilbert space.

This means that variation of output signal of operator is bounded by diffeomorphism of input signal. Invariant operator to transform $Lf(x)$ of function $f(x)$ (e.g., translation: $L_c f(x) = f(x - c)$) is operator that satisfy the condition [33]: $\Phi(Lf) = \Phi(f)$. Output signal does not depend on transform of input signal. For example, modulus of Fourier transform is translation invariant, but is instable to deformations at high frequencies. Wavelet transform satisfies condition (2), but is not invariant to translations and rotations. Non-linear operator resolves this problem [33].

Informative features. Here we used Matlab implementation of Mallat scattering transform [36]. Wavelets with three degrees of freedom (translations along both axes and rotation) were used. Default setting of framework were applied. Variance of each coefficient was used as informative features [34]. Vector of features was of 701 elements length. High accuracy of classification of images of hand-written digits have been demonstrated [34].

Appendix B

Support Vector Machine (SVM). SVM is a linear supervised learning classification algorithm. It requires training set of n points: $(X_1, y_1), \dots, (X_n, y_n)$, where X_i is p -dimensional vector of data points, $y_i = \{1; -1\}$ is label that indicate class of the current data vector. The p -dimensional feature space is divided by hyperplane that is assigned by its normal vector ω that should be found. It the task can be solved using the following equation:

$$\omega^T X_i + b = 0, \quad (4)$$

where superscript T denotes transpose.

Such classifier can margin only linearly separable data with no observation errors. If elements cannot be accurately divided on both side of plane, this leads to optimization problem. If classes are linearly nonseparable, so called kernel trick should be used. The approach is to map feature space to another of higher dimensionality, where the data can be separated by hyperplane. Finally, the task can be formulated [37]:

$$0.5 \|\omega\|^2 + C \sum_{i=1}^l \xi_i \rightarrow \min_{\omega, b, \xi} \quad \text{subject to } y_i(\omega^T \varphi(X_i) + b) \geq 1 - \xi_i, \quad \xi_i \geq 0, \quad i = 1, \dots, l, \quad (5)$$

where $\varphi(X_i)$ maps X_i into a higher-dimensional space;

$C > 0$ is the regularization parameter.

The decision function is [37]: $f = \text{sign}(\omega^T \varphi(X) + b)$.

In SVM implementation [37], used in this paper, parameters of classifier C and kernel γ are selected automatically using “grid-search” and cross-validation (CV) [38]. In ν -fold CV, training set is divided into ν subsets. One of them is selected for testing, classifier has been trained using all remained. Accuracy of classification is compared in each case, the best classifier is selected. This procedure is needed to avoid overfitting problem. Accuracy of cross-validated classifiers is compared for each pair of values of C and γ . In this paper we trained and tested all classifiers at independent set. Quarter of full dataset is randomly selected and used as training set with 5-fold CV (if number of elements is enough).

Multi-class classification is implemented as “one-against-one” approach. In the case of k classes $k(k-1)/2$ binary classifiers are constructed [37]. Each classification is considered to be vote, designated class is one having maximum votes [37].

Accuracy. Accuracy of binary classification is characterized by four values: true positive (TP), true negative (TN), false positive (FP, type I error), false negative (FN, type II error). Total accuracy can be expressed in various ways. Accuracy (6) is widely used and is estimated in this paper [39]:

$$\text{Accuracy} = (\text{TP} + \text{TN}) / (\text{TP} + \text{TN} + \text{FP} + \text{FN}). \quad (6)$$

Sense of this value is ratio between correctly classified samples and their total number. Overall accuracy estimated as mean of accuracies of all classes.

Preprocessing of data. Preliminary scaling of train and testing data is important for classification tasks [38]: it can prevent domination of features in greater numeric ranges and reduce difficulties during calculation. All features should be restricted to the similar range. Increasing of accuracy after scaling has been demonstrated [38]. The similar scaling coefficients should be used for training and testing set [38]. The simplest

solution is min-max: subtract minimum value and divide by maximum. The data is restricted to [0; 1] range. Standardization can reduce influence of noise and outliers: the feature mean is subtracted from each of them, then every feature is divided by its STD. In this paper we used median instead of mean that is additionally reduces sensitivity to outliers.

REFERENCES

1. Ghafari, S.H. A Fault Diagnosis System for Rotary Machinery Supported by Rolling Element Bearings / S.H. Ghafari.
2. Jordan, M.A. Paper about orbit plots / M.A. Jordan // *Orbit*. – 1993.
3. Shirman, A.R. Practice of vibrational diagnosing and monitoring of equipment state/ A.R. Shirman, A.B. Solovyov. – Moscow : Nauka, 1996. – 276 p. (in Russian)
4. *Vibrational diagnosing / Ye.Z. Madorskiy [et al.] ; ed. G.Sh. Rosenberg*. – St. Petersburg : Federal State educational establishment, 2003. – 284 p. (in Russian)
5. Rusov V.A. Spectral vibrational diagnosing / V.A. Rusov. – Perm : Vibro-center LLC, 1996. – 215 p. (in Russian)
6. Rusov V.A. Diagnosing of defects of rotary equipment relying on vibrational signals / V.A. Rusov. – Perm, 2012. (in Russian)
7. Aherwar, A. Vibration analysis techniques for gearbox diagnostic: A review / A. Aherwar, S. Khalid // *Int J Adv Eng Technol*. – 2012. – Vol. 3. – P. 4–12.
8. Sait, A.S. A Review of Gearbox Condition Monitoring Based on vibration Analysis Techniques Diagnostics and Prognostics / A.S. Sait, Y.I. Sharaf-Eldeen // *Rotating Machinery, Structural Health Monitoring, Shock and Vibration, Volume 5 : Conference Proceedings of the Society for Experimental Mechanics Series / Springer ; ed. T. Proulx*. – New York, NY, 2011. – P. 307–324.
9. Bechhoefer, E. A Review of Time Synchronous Average Algorithms / E. Bechhoefer, M. Kingsley. – 2009. – P. 10.
10. Zhang, X. A new time synchronous average method for variable speed operating condition gearbox / X. Zhang, G. Wen, T. Wu // *J. Vibroengineering*. – 2012. – Vol. 14, № 4. – P. 1766–1774.
11. Kechik, D. Segmented Autoregression Pitch Estimation Method / D. Kechik, I. Davydov // *2020 International Conference on Dynamics and Vibroacoustics of Machines (DVM) : 2020 International Conference on Dynamics and Vibroacoustics of Machines (DVM)*. – 2020. – P. 1–6.
12. Al-Khazali, H.A.H. Geometrical and Graphical Representations Analysis of Lissajous Figures in Rotor Dynamic System / H.A.H. Al-Khazali // *IOSR J. Eng.* – 2012. – Vol. 02, № 05. – P. 971–978.
13. Gavrilov A.M. Studying of Lissajous figures for measuring of phase relations in spectrum of triharmonic signal / A.M. Gavrilov, R.O. Sitnikov // *University news. North-caucasian region. Technical sciences series*. – 2006. – No. 3. – P. 34–39. (in Russian)
14. Genkin, M.D. Vibroacoustic diagnostics of machines and mechanisms / M.D. Genkin, A.G. Sokolova. – Moscow : Mashinostroenie, 1987. – 288 p. (In Russian)
15. Kosmach, N.V. Approach of vibrational diagnosing of rolling bearing / N.V. Kosmach, Yu.P. Aslamov. – 2020.
16. Rotating Machinery Diagnostics Using Deep Learning on Orbit Plot Images / H. Jeong [et al.] // *Procedia Manuf.* : 44th North American Manufacturing Research Conference, NAMRC 44, June 27 – July 1, 2016, Blacksburg, Virginia, United States. – 2016. – Vol. 5. – P. 1107–1118.
17. Polar and Orbit Plot Analysis for Unbalance Identification in A Rotating System / A. Sen [et al.] // *IOSR J. Mech. Civ. Eng.* – 2017. – Vol. 14, № 03. – P. 49–56.
18. Orbit Analysis For Imbalance Fault Detection In Rotating Machinery / C. Costa [et al.] // *IOSR J. Electr. Electron. Eng. IOSR-JEEE*. – 2018. – Vol. 13. – P. 43–53.
19. Goldin, A.S. *Vibration of rotary machines / A.S. Goldin*. – Moscow : Mechanical engineering, 1999. – 344 p. (in Russian)
20. Buscarello, R.T. *Practical Solutions to Machinery and Maintenance Vibration Problems / R.T. Buscarello*. – Pub. Fifth edition. – Update international Inc., 2011. – 262 p.
21. Kechik, D.A. Vibrational signal power variance compensation during equipment speed mode changing / D.A. Kechik // *Doklady BGUIR*. – 2020. – Vol. 18, No 5. – P. 27–34.
22. Bently, D.E. *Fundamentals of Rotating Machinery Diagnostics / D.E. Bently, C.T. Hatch*. – ASME, Bently Pressurized Bearing Company, 2002. – 726 p.
23. Scheffer, C. *Practical Machinery Vibration Analysis and Predictive Maintenance / C. Scheffer, P. Girdhar*. – Elsevier, 2004. – 263 p.
24. Kechik, D. Shaft Misalignment Data for: Inter-component Phase Processing of Quasipolyharmonic Signals / D. Kechik, Y. Aslamov, I. Davydov. – 2020. – DOI: 10.17632/pt9mjcvghd.1.
25. Kechik, D. Shaft Angular Misalignment Dataset / D. Kechik, Y. Aslamov, I. Davydov. – 2021. – DOI: 10.17632/kf96jx9dzf.1.
26. Barkov, A.V. Monitoring and diagnostics of rotary equipment relying on its vibration / A.V. Barkov, N.A. Barkova, A.Yu. Azovtsev. – St. Petersburg : SMTU, 2000. – 159 p. (in Russian)
27. Barkov, A.V. *Vibrational diagnosing of machines and equipment. Analysis of vibration. Tutorial / Barkov, N.A. Barkova*. – St. Petersburg : SMTU, 2004. – 156 p. (in Russian)
28. Influence of changes in shaft rotational speed of rotary equipment on frequency-domain processing / Yu.P. Aslamov [et al.] // *Doklady BGUIR*. – 2018. – Vol. 113, No 13. – P. 13–18.
29. Voskoboynikov, Y.E. Filtration of signals and images: Fourier and wavelet algorithms (with examples in Mathcad) / Y.E. Voskoboynikov, A.V. Gochakov, A.B. Kolker. – Novosibirsk : NGASU (Sibstrin), 2010. – 188 p. (In Russian)
30. Kechik, D. Shaft orbits dataset: parallel and angular misalignment / D. Kechik, I. Davydov. – 2021. – DOI: 10.17632/8b33tx79wt.1.

31. Vorobiov, V.I. Inter-component phase processing of quasipolyharmonic signals / V.I. Vorobiov, D.A. Kechik, S.Y. Barysenka // Appl. Acoust. – 2021. – Vol. 177. – 14 p.
32. Barysenka, S.Y. Single-channel speech enhancement using inter-component phase relations / S.Y. Barysenka, V.I. Vorobiov, P. Mowlae // Speech Commun. – 2018. – Vol. 99. – P. 144–160.
33. Mallat, S. Group Invariant Scattering / S. Mallat // Commun. Pure Appl. Math. – 2012. – Vol. 65, № 10. – P. 1331–1398.
34. Bruna, J. Invariant Scattering Convolution Networks / J. Bruna, S. Mallat // IEEE Trans. Pattern Anal. Mach. Intell. – 2013. – Vol. 35, № 8. – P. 1872–1886.
35. Oyallon, E. Deep roto-translation scattering for object classification / E. Oyallon, S. Mallat // IEEE. – 2015. – P. 2865–2873.
36. ScatNet: a MATLAB Toolbox for Scattering Networks [Electronic resource]. – Mode of access: <https://github.com/scatnet/scatnet/blob/master/doc/impl/impl.pdf>. – Date of access: 11.10.2020.
37. Chang, C.-C. LIBSVM: A library for support vector machines / C.-C. Chang, C.-J. Lin // ACM Trans. Intell. Syst. Technol. – 2011. – Vol. 2, № 3. – 27 p.
38. Hsu, C.-W. A practical guide to support vector classification / C.-W. Hsu, C.-C. Chang, C.-J. Lin // Journal of Data Analysis and Information Processing. – 2003. – Vol. 8, № 2. – P. 16.
39. Tharwat, A. Classification assessment methods / A. Tharwat // Applied Computing and Informatics. – 2020. – Vol. 17, № 1. – P. 168–192.

Поступила 24.02.2021

АЛГОРИТМ КЛАССИФИКАЦИИ ОРБИТ ВАЛА

Д.А. КЕЧИК, И.Г. ДАВЫДОВ, И.В. ЛОЩИНИН, К.Д. ЖУКОВСКИЙ

В настоящей работе рассматривается классификация пространственных шаблонов орбиты вала. Опробовано применение современных методов обработки сигналов (метод спектральной интерференции и рассеивающее преобразование Малла) в задаче получения пространственных шаблонов, извлечения информативных признаков и классификации. Рассматривалась сильная зависимость пространственных шаблонов от флуктуаций параметров сигнала и непостоянство их формы. Оценивалась эффективность классификации пространственных шаблонов при использовании различных подходов в ходе численного эксперимента и натурального моделирования. Рассмотрена предобработка сигнала и извлеченных информативных признаков. Предложен подход к различению типа и степени выраженности расцентровки валов, основанный на частоте встречаемости различных классов пространственных шаблонов, показана эффективность подхода.

Ключевые слова: *распознавание образов, частотная область, пространственная область, синхронное усреднение, фазовая обработка, вибрационная диагностика, рассеивающее преобразование, вейвлет-преобразование, сверточная сеть, машина на опорных векторах.*